Available online at www.sciencedirect.com
SCIENCE DIRECT®
Composites Science and Technology 65 (2005) 1719–1727
COMPOSITES SCIENCE AND TECHNOLOGY
www.elsevier.com/locate/compscitech

Prediction and three-dimensional Monte-Carlo simulation for tensile properties of unidirectional hybrid composites

Martin Y.M. Chiang [a,*], Xianfeng Wang [a], Carl R. Schultheisz [a,b], Jianmei He [a,c]

[a] Polymers Division, National Institute of Standards and Technology, Gaithersburg, MD 20899-8544, USA
[b] National Transportation Safety Board, Washington, DC 20594, USA
[c] Japan Aerospace Exploration Agency (JAXA), Japan

Received 28 October 2004; received in revised form 21 February 2005; accepted 23 February 2005
Available online 27 April 2005

Abstract

A 3D fiber tow-based analytical model incorporating shear-lag theory and a statistical strength distribution has been used to simulate the tensile properties and predict the tensile strength of unidirectional hybrid composites. Also, we have developed an expression of interfacial shear stress between tows for the simulation. The hybrid composites considered in this study contain two different types of fiber tows (glass/epoxy and carbon/epoxy tows) that are intimately mixed in a random pattern throughout the composite. The tow is defined as a fiber/matrix system (an impregnated tow) rather than a bundle of fibers. The properties of the tows used in the analytical model are derived using the rule-of-mixtures from the properties of the constituent materials and their volume fractions. For low levels of carbon fiber reinforcement, the low strain to failure of the carbon fibers can initiate failure and actually have a detrimental effect on strength. Otherwise, the study indicates that there are no synergistic effects of hybridization on the tensile properties, which consequently can be described for the most part using the rule-of-mixtures.

Keywords: Hybrid composites; Monte-Carlo simulation; Rule-of-mixtures; Tensile properties

1. Introduction

The development of composites containing more than one type of fiber reinforcement (hybrid composites) is motivated by the ability to combine advantageous features of various fiber systems – improved performance as well as reduced weight and cost. Understanding how the mechanical properties of hybrid composites depend on the constituents is important in approaching the design requirements or in developing new hybrid materials. To a large extent, these material properties must be determined experimentally, so that if a change in the hybrid composite design parameters is required, a high cost in time and materials is incurred. Therefore, an analytical model or simulation is needed to predict the properties of hybrid composites as a function of their constituent properties. Two and three-dimensional Monte-Carlo simulation techniques coupled with the classical or modified shear-lag models have been widely used for predicting the tensile properties of unidirectional non-hybrid composites [1–4]. Also, the Monte-Carlo study has been extended to intraply hybrid composites that are formed by laying up prepreg sheets containing different reinforcing fibers (macrocombination) [5,6]. All of these simulations considered several individual fibers embedded in matrix and their interface with the matrix in a limited representative volume element (an ultra-small composite), which might not extrapolate to the properties of a macro-composite. A weak-link scaling technique was suggested to

* Corresponding author. Tel.: +1 301 975 5186; fax: +1 301 975 4977.
E-mail address: martin.chiang@nist.gov (M.Y.M. Chiang).

0266-3538/$ - see front matter © 2005 Elsevier Ltd. All rights reserved.
doi:10.1016/j.compscitech.2005.02.012

extrapolate the simulated strength of a small composite to a macro-composite [7]. In the early 1990s, an analytical model based on the concept of global load redistribution upon fiber fracture was developed to predict ultimate strength of ceramic–matrix composites [8]. The numerical simulations have also been performed to demonstrate the predictions.

The hybrid composites (or hybrids) considered in this study contain different types of fiber tows (glass/epoxy tows and carbon/epoxy tows) that were intimately mixed throughout the resin matrix, without preferred concentration of either type of fiber. This true blended reinforcement (microcombination) will affect the composite micromechanics, and the difference in mechanical behavior between such a hybrid and non-hybrid or intraply hybrid reinforcements may be appreciable. Therefore, in this study, both a tow-based analytical model and a tow-based 3D simulation (Monte-Carlo method with the modified shear-lag theory) are developed to predict tensile properties and simulate the tensile behavior of unidirectional hybrid composites. The tow-based model/simulation is defined to mean that the tow is treated as a minimal microstructure, and necessary material properties input for the model/simulation are based on the tow properties. The tow itself is a fiber/matrix system (an impregnated tow) rather than a bundle of fibers. The interfacial shear strength between tows is assumed to be the shear strength of the matrix. Thus, it is a two-phase instead of a three-phase model.

The advantage of the tow-based Monte-Carlo simulation is that the simulated composite size can be much larger, so that it becomes more representative of a real composite (macro-composite) without using any scaling techniques. This work is limited to a model hybrid composite material with unidirectional glass and carbon fiber systems in an epoxy matrix. The glass fibers have a lower stiffness than the carbon fibers, but have better strain at failure and are relatively inexpensive, while the carbon fibers are stiff and have higher strength, but are relatively expensive. The fiber content plays a major role in the stress distribution of composites; therefore, the hybrid composition (α, defined as the volume fraction of carbon/epoxy tows out of the total fiber/epoxy tows in the hybrid composite) is set as the primary variable of interest, with the epoxy matrix content held fixed. A few simulations were also performed using different values of the epoxy volume fraction with fixed hybrid composition to assess the effect of varying this parameter on the tensile properties of the hybrid composites.

2. Tow-based simulation method

The theoretical and computational background for the present study will be outlined briefly. First, a tow-based 3D shear-lag model for the equilibrium of a tow segment associated with the Monte-Carlo simulation will be established. Also, the description of interfacial shear stress between tows will be developed for the simulation. Second, the solution method in solving the equilibrium equations will be discussed. The Monte-Carlo simulation procedure will form the last part of this section. Linearly elastic behavior is assumed in all cases.

2.1. Tow-based 3D shear-lag model and interfacial shear stress between tows

In the simulation, the unidirectional hybrid composite (carbon/glass/epoxy, Fig. 1) under a tensile deformation (u_0) in the longitudinal direction is composed of $I \times J$ impregnated tows, and these tows are arranged in square arrays (Fig. 2(a)). For the numerical differentiation required in the simulation, each tow of the composite is partitioned into K segments of length Δz along the longitudinal direction of the tow, which has total length L (Fig. 2(b)). Therefore, considering the equilibrium of each tow segment (Fig. 3(a)) based on the assumption in the shear-lag model [2,3], one can obtain the governing equation of the equilibrium in the following form:

$$EA\frac{\mathrm{d}^2u}{\mathrm{d}z^2} + d\sum_{l=1}^{4}\tau^l = 0, \tag{1}$$

where E, A and d are the modulus, cross-sectional area and size of the tow, respectively; u is the displacement

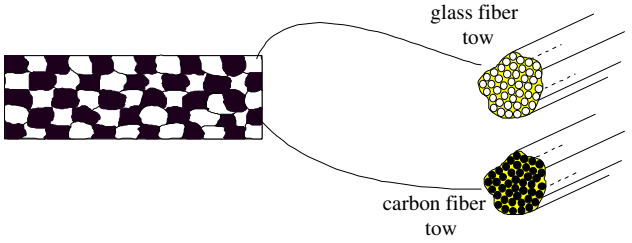

Fig. 1. Schematic cross-section of tow-based unidirectional hybrid fiber composites.

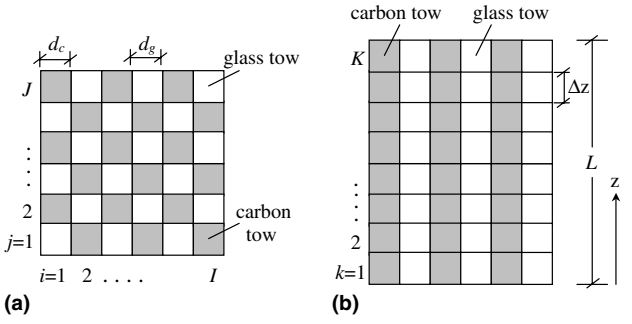

Fig. 2. Side view (a), and top view (b) of the hybrid composite (a square array model). d_c and d_g are the size of carbon and glass tows, respectively.

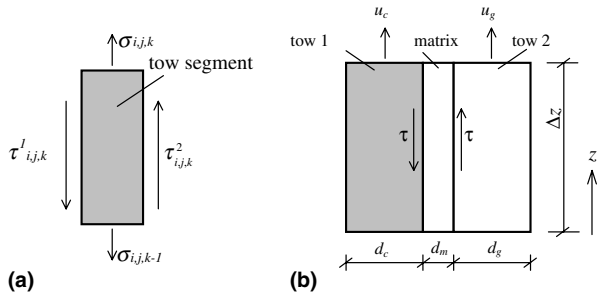

Fig. 3. Free-body diagram of a tow segment (a), and representative segments for the shear stress analysis in the simulation (b).

of the tow segment in the longitudinal direction; τ is the interfacial shear stress determined by the relative displacement between the tow and its adjacent tows; and l ranges from 1 to 4 since a square array is considered.

Based on a representative segment of the composite (Fig. 3(b)), the interfacial shear stress between a tow and matrix (τ) can be written as follows:

$$\tau_{1/\mathrm{m}} = G_1(u_1 - u_{1/\mathrm{m}})/\frac{d_1}{2} = G_{\mathrm{m}}(u_{1/\mathrm{m}} - u_{\mathrm{m}})/\frac{d_{\mathrm{m}}}{2}, \tag{2}$$

$$\tau_{\mathrm{m}/2} = G_{\mathrm{m}}(u_{\mathrm{m}} - u_{\mathrm{m}/2})/\frac{d_{\mathrm{m}}}{2} = G_2(u_{\mathrm{m}/2} - u_2)/\frac{d_2}{2}, \tag{3}$$

where the subscript 1, 2, and m correspond to tow 1, tow 2, and matrix as shown in Fig. 3(b). G is the shear moduli. u_1, u_2 and u_{m} are the displacements at the centerlines of the tow 1, tow 2 and matrix, respectively. $u_{1/\mathrm{m}}$, $u_{\mathrm{m}/2}$ are the displacement at the tow 1/matrix and matrix/tow 2 interfaces. d_1 and d_2 are the tow size; d_{m} is the distance between two adjacent tows. Both tow 1 and tow 2 can be either glass tows or carbon tows based on the configuration. By assuming the shear stresses at left- and right-hand sides are equal (i.e., $\tau_{1/\mathrm{m}} = \tau_{\mathrm{m}/2} \equiv \tau$), and solving the simultaneous Eqs. (2) and (3) to eliminate the parameters $u_{1/\mathrm{m}}$, $u_{\mathrm{m}/2}$ and u_{m}, one can obtain the interfacial shear stress (τ) as

$$\tau = \frac{2G_1G_2G_{\mathrm{m}}(u_1 - u_2)}{G_1G_{\mathrm{m}}d_2 + 2G_1G_2d_{\mathrm{m}} + G_2G_{\mathrm{m}}d_1}. \tag{4}$$

If $G_{\mathrm{m}} \ll G_1$ and G_2, the interfacial shear stress of Eq. (4) can be further reduced to the classical shear-lag stress [9] as

$$\tau \approx \frac{G_{\mathrm{m}}(u_1 - u_2)}{d_{\mathrm{m}}}. \tag{5}$$

In the current tow-based 3D Monte-Carlo simulation, d_m is set to be zero. Therefore, the τ of Eq. (1) is expressed in the following form:

$$\tau = \frac{2G_1G_2(u_1 - u_2)}{G_1d_2 + G_2d_1}. \tag{6}$$

This description of interfacial shear stress, which is different from that used in conventional shear-lag models, will be incorporated into the proposed tow-based Monte-Carlo simulation. Also, it is noted that G_{m} is not present in the Eq. (6), since its effect on τ is already factored in through the impregnated fiber tows in the simulation.

2.2. Solution method

Let the displacement for the segment (i, j, k) be denoted as $u_{i,j,k}$ with $1 \leqslant i \leqslant I$, $1 \leqslant j \leqslant J$ and $1 \leqslant k \leqslant K$ (Fig. 2). Then, the differentiation of Eq. (1) can be rewritten using the following finite difference form [1]:

$$\frac{\mathrm{d}^2u_{i,j,k}}{\mathrm{d}z^2} = \frac{u_{i,j,k-1} - 2u_{i,j,k} + u_{i,j,k+1}}{(\Delta z)^2}, \tag{7}$$

where the segment length (Δz) is usually chosen as the magnitude of ten times the tow size [5,6]. When the rupture of a tow segment occurs, Eq. (7) will change to [10]:

$$\frac{\mathrm{d}^2u_{i,j,k}}{\mathrm{d}z^2} = \frac{4\{H_{i,j,k+1}(u_{i,j,k+1} - u_{i,j,k}) - H_{i,j,k}(u_{i,j,k} - u_{i,j,k-1})\}}{(2 + H_{i,j,k+1} + H_{i,j,k})(\Delta z)^2} \tag{8}$$

with

$$H_{i,j,k} = \begin{cases} 0, & \text{for} \quad \sigma_{i,j,k} > X_{i,j,k}, \\ 1, & \text{for} \quad \sigma_{i,j,k} \leqslant X_{i,j,k}, \end{cases} \tag{9}$$

where $\sigma_{i,j,k}$ and $X_{i,j,k}$ are the normal stress and the tensile strength of the tow segment, respectively.

When the interfacial shear stress of the tow segment ($\tau_{i,j,k}$) exceeds the interfacial shear strength (τ_{m}), debonding will occur at the interface, and τ_{m} will subsequently become the friction stress (τ_{s}) at the debonded interface. Thus, substituting Eq. (8) into Eq. (1), we have

$$\frac{4E\,A\{H_{i,j,k+1}(u_{i,j,k+1} - u_{i,j,k}) - H_{i,j,k}(u_{i,j,k} - u_{i,j,k-1})\}}{(2 + H_{i,j,k+1} + H_{i,j,k})(\Delta z)^2} + d\sum_{l=1}^{4}\left\{\tau^l_{i,j,k}(1 - P^l_{i,j,k}) + P^l_{i,j,k}\zeta^l_{i,j,k}\tau_{\mathrm{s}}\right\} = 0 \tag{10}$$

with

$$P^l_{i,j,k} = \begin{cases} 0, & \text{if } |\tau| \leqslant \tau_{\mathrm{m}}, \\ 1, & \text{if } |\tau| \geqslant \tau_{\mathrm{m}}, \end{cases} \tag{11}$$

where the parameter $\zeta^l_{i,j,k}$ determines the slide direction, its value is either 1 or -1 according to the sign of the difference in the displacement between the corresponding neighboring segments [11]. By incorporating appropriate boundary conditions, Eq. (10) can be solved using the successive over-relaxation method [12] to obtain the displacement field of a boundary-value problem. The normal stress of the segment (i, j, k) can be obtained through the following equation:

$$\sigma_{i,j,k} = E\frac{u_{i,j,k} - u_{i,j,k-1}}{\Delta z}. \tag{12}$$

Also, the average applied stress (σ_{app}) exerted at the end of the specimen (where $k = K$) is given by:

$$\sigma_{app} = \frac{1}{I \times J} \sum_{i=1}^{I} \sum_{j=1}^{J} \sigma_{i,j,K}. \tag{13}$$

2.3. Monte-Carlo simulation procedure

In the Monte-Carlo simulation, the tow strength is statistically described by the two-parameter Weibull distribution [12]:

$$F(X) = 1 - \exp\left\{ -\frac{l}{l_0} \left(\frac{X}{\sigma_0} \right)^{\beta} \right\}, \tag{14}$$

where $F(X)$ is the probability that the tow strength is less than or equal to X; σ_0 and β are the Weibull scale and shape parameters, respectively. Note that l_0 is the original gage length at which the fiber tow tension test and the evaluation of Weibull parameters are conducted. l is the tow length of interest and is taken as the segment length (Δz) of Eq. (7). The simulation procedure, in general, can be described as follows:

(1) Based on Eq. (14), the strength of each tow segment ($X_{i,j,k}$) with the length Δz is allocated as

$$X_{i,j,k} = \sigma_0 \left[-\frac{l_0}{\Delta z} \ln(1 - F) \right]^{1/\beta}, \tag{15}$$

where the distribution function F is a uniformly distributed random number ranging from 0 to 1.

(2) A uniform initial displacement field (u_0) is applied longitudinally at the boundary of the hybrid, and the displacement of tow segment ($u_{i,j,k}$) is obtained through Eq. (7) using the successive over-relaxation algorithm; the interfacial and normal stresses associated with the tow segment are calculated from Eqs. (6) and (12) afterwards.

(3) Determine whether a tow break or interfacial debonding of the tow segment has occurred. If not, go to step 4. Otherwise, the governing equation is resolved taking the breakage or debonding into account. This step is repeated until equilibrium is achieved for the current applied displacement.

(4) Increase the displacement with Δu, and repeat steps (2) and (3). An apparent stress/strain curve can be constructed up to the rupture of the composite when the stress drops suddenly, and the simulation process ends.

3. Results and discussion

Both carbon and glass tows were treated as two-phase material systems with epoxy matrix and their corresponding fibers. The longitudinal moduli (E) required in the Monte-Carlo simulation for each type of tow were calculated from the rule-of-mixtures: $E = v_f E_f + v_m E_m$, based on the constituent properties (reported mean values from the literature) listed in Table 1 [13,14]. v_f and v_m are the volume fractions of fiber and matrix, respectively; E_f and E_m are the Young's modulus of fiber and matrix, respectively. The shear modulus of the tow (G) was obtained through a modified rule-of mixtures because of the Poisson's effect between the fiber and matrix [15,16] as follows:

$$\frac{1}{G} = \frac{1}{v_f + \eta_s v_m} \left(v_f \frac{1}{G_f} + \eta_s v_m \frac{1}{G_m} \right) \tag{16}$$

with

$$\eta_s = \frac{1}{2} \left(1 + \frac{G_m}{G_f} \right), \tag{17}$$

where G_f and G_m are the shear modulus of the fiber and matrix, respectively. The calculated tow properties for different fiber volume fractions are listed in the Table 2.

The strengths of the epoxy-impregnated carbon tows are described with the Weibull statistical distribution, but the strength of the epoxy-impregnated glass tows are assumed to be a constant value (equal to the strength of glass/epoxy composite) [16] since the variability of the strength of glass fiber tows is usually small compared to that of carbon fiber tows (the Weibull shape factor of

Table 1
Moduli of tow constituents

Properties	Carbon	Glass	Matrix
Elastic modulus (GPa)	230.0	76.0	3.4
Shear modulus (GPa)	28.8	29.98	1.26

Table 2
Moduli of tows corresponding to different fiber volume fractions

Mechanical properties of tows	Fiber volume fraction							
	50%		60%		70%		75%	
	Carbon	Glass	Carbon	Glass	Carbon	Glass	Carbon	Glass
Elastic modulus (GPa)	116.7	39.7	139.4	47.0	162.0	54.2	173.4	57.9
Shear modulus (GPa)	3.4	3.4	4.4	4.4	5.8	5.8	6.8	6.9

Table 3
Material parameters associated with the strength of tows

Material parameters	Fiber volume fraction			
	50%	60%	70%	75%
Weibull scale parameter of carbon tow, σ_0 (GPa)	1.49	1.79	2.09	2.24
Weibull shape parameter of carbon tow, β	15.0	15.0	15.0	15.0
Strength of glass tow (GPa)	0.82	0.97	1.13	1.21
Cross-section[a] area (mm^2)	0.41	0.34	0.29	0.27

[a] Cross-section area is calculated based on 6000 fibers.

glass tows is much greater than 20). Both tows are assumed to have the same cross-sectional area. Table 3 provides the parameters relevant to the strength and geometry of tows for the different fiber contents used in simulations. In the table, the Weibull scale and shape parameters (σ_0 and β) of the carbon tows and the constant strength of the glass tows (S_g) with 60% fiber volume fraction (v_f) were obtained from the literature [17,18]. The β was assumed to be independent of v_f. For the v_f other than 60%, σ_0 was estimated proportionally, and S_g was derived based on the following equation [19]:

$$S_g = s_{gf} v_{gf} + (\sigma_m)_{\varepsilon@2\%}(1 - v_{gf}), \quad (18)$$

where $(\sigma_m)_{\varepsilon@2\%}$ is the matrix stress corresponding to a strain of 2% (since it is assumed that the strain at failure of the glass tow is 2%). s_{gf} is the strength of the glass fiber and equals 1.57 GPa, which is evaluated through Eq. (18) by setting $S_g = 0.97$ GPa, $v_{gf} = 60\%$, and $(\sigma_m)_{\varepsilon@2\%} = 0.068$ GPa obtained from the literature [18]. The interfacial shear strength (τ_m) between tows was assumed to be equal to the shear strength of epoxy (42 MPa). The friction stress (τ_s) at debonded interfaces is assumed to be 10 MPa [7].

In order to validate the proposed tow-based Monte-Carlo simulation, a predicted tensile strength from a simulation for a unidirectional carbon fiber reinforced polymeric (CFRP) composite was compared with existing experimental measurements reported in the literature [20]. The discrepancy between the prediction and the measurement is less than 1%. The simulation of the CFRP composite (non-hybrid composite) was achieved by setting the glass tow properties to be the same as the carbon tow properties. Also, if the parameter J (Fig. 2) is set to be equal to one, a 2D simulation can be obtained. It is found that the discrepancy in the predicted tensile strength between the 2D and 3D simulations of CFRP is about 7%, with the 2D result being lower than that of the 3D result. This is reasonable since the 2D simulation gives a higher stress concentration at a broken tow than does the 3D simulation [4]. In performing a calculation, the number of tows (I, J and K) in the simulation should be large enough to make the simulation more representative for the statistical distribution of tow strength. Fig. 4 shows the predicted tensile

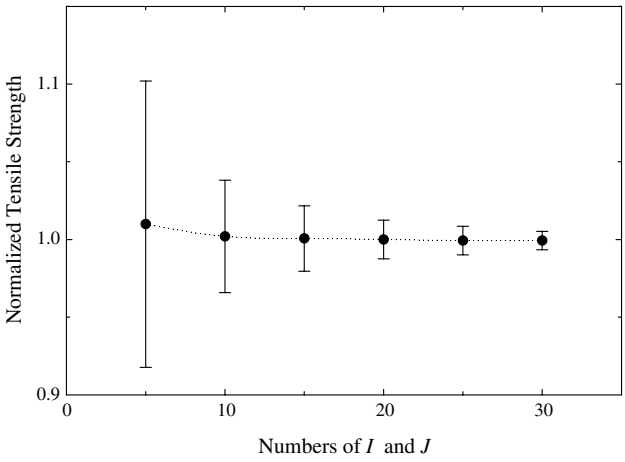

Fig. 4. Predicted tensile strength as function of tow numbers in i- and j-directions. The error bars represent the standard uncertainty from a distribution of results due to the statistical strength distribution of carbon tows.

strength of the CFRP from 3D simulations as a function of number of tows in the i and j-directions, where the number of tow segments (K) in the k-direction is set to be 50 (see Fig. 2). It is found that the maximum deviation from a distribution of results (error bars, Fig. 4), due to the statistical strength distribution of carbon tows, approaches to a stationary value when the magnitudes of I and J are beyond 30. Therefore, in simulations for predicting the strength of hybrid composites, the values for I and J were also chosen to be 30 and $K = 50$ so that the simulated composite size is comparable to a specimen size normally used in experiments.

Comparisons were also made between values determined from the Monte-Carlo simulation and previously reported values [16] for the moduli of hybrid composites with two different hybrid contents ($\alpha = 0.34$ and 0.62). The previously reported values were obtained through finite element analyses (FEA) and experimental measurement. Typical images of the hybrid composites used in the experiments are shown in Fig. 5. The simulated, FEA and experimental results for both hybrid contents are listed in Table 4. The calculated moduli agree quite well, validating the Monte-Carlo tow-based simulation of hybrid composite behavior.

The hybrid composition (α) was set as a variable ranging from 0% to 100% to examine the effect of hybridization on the tensile properties. For $\alpha = 0\%$, the composite corresponds to a non-hybrid glass/epoxy composite (GFRP), and for $\alpha = 100\%$, the composite corresponds to a non-hybrid carbon/epoxy composite (CFRP). For most of the simulations, we assumed that the volume fraction of epoxy matrix in both the glass/epoxy and carbon/epoxy tows is 40%, while the hybrid composition α was varied. This implies that the total volume fraction of the epoxy matrix in the hybrid composites is also 40%. Some other values of epoxy volume

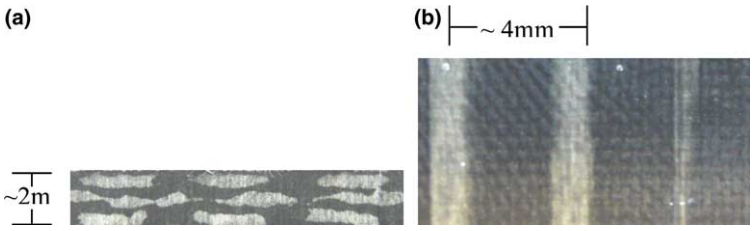

Fig. 5. Typical micrographs of hybrid composite samples: cross-section (a), surface (b); the bright regions represent the glass/epoxy fiber tows and the dark regions represent the carbon/epoxy fiber tows.

Table 4
Comparisons of hybrid composites modulus

Modulus	$\alpha = 0.34$ (GPA)			$\alpha = 0.62$ (GPA)		
	Monte-Carlo Simulation (3D)	3D FEA	Exp.	Monte-Carlo Simulation (3D)	3D FEA	Exp.
E	90.8	90.2	83.3	120.7	122.0	101.6

fraction with a fixed hybrid composition were also examined in simulations to assess the importance of this parameter.

Fig. 6 presents a typical simulated stress–strain relationship for composites with different hybrid compositions ($\alpha = 0.5$ and 1). Also shown in the figure is the segment failure density, which is defined as the ratio of failed tow segments to the total tow segments ($I \times J \times K$) in the simulation, as a function of applied strain. The failure of a tow segment is indicated as either an interfacial failure with adjacent tow segments or as a tensile failure of the tow segment. One can note that, when $\alpha = 0.5$ (Fig. 6(a)), the number of failed segments is much higher than when $\alpha = 1$ (Fig. 6(b)). This is because the stress intensity induced at a broken tow in a non-hybrid composite (such as $\alpha = 1$) is lower than that in a hybrid composite [21]. Also, the simulations indicate that more segments in the hybrid composite fail at the interface rather than through direct tension. In contrast, for the non-hybrid composite, fewer segments fail at the interface rather than in tension at lower strains, but there is an abrupt increase of segments failing along the interface near the composite rupture point. These trends continued in the simulations with different hybrid compositions.

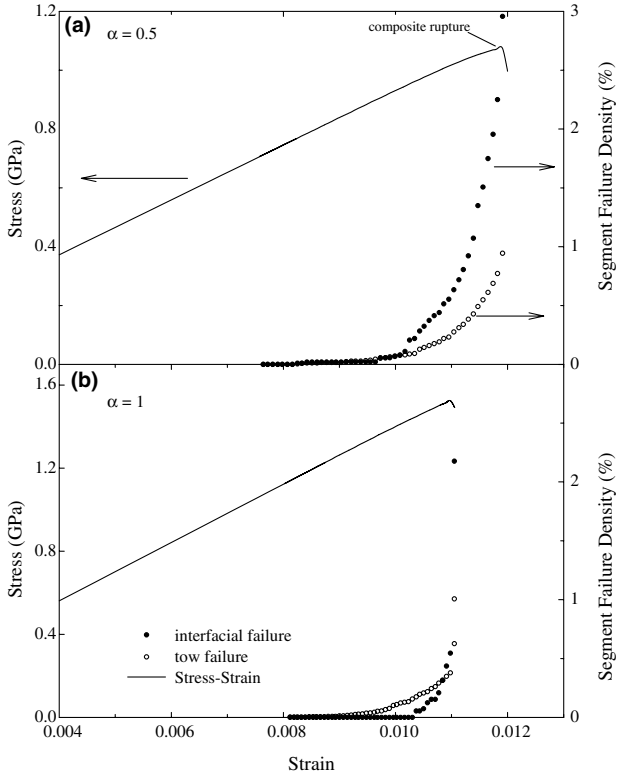

Fig. 6. Typical simulated stress–strain relationship and the segment failure density as a function of applied strain for $\alpha = 0.5$ (a), and $\alpha = 1$ (b).

Fig. 7 shows the simulated longitudinal modulus (symbols) obtained from the stress–strain curve (shown in Fig. 6) as a function of hybrid composition. The solid

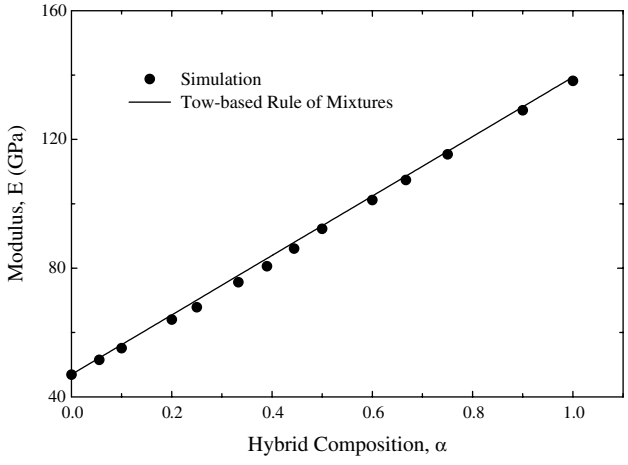

Fig. 7. Comparison of modulus between the results obtained from the simulation and the tow-based rule of mixtures as a function of hybrid composition.

line is the result from a tow-based rule of mixtures, which is defined as: $E = E_{ct}\alpha + E_{gt}(1-\alpha)$. E_{ct} and E_{gt} are the moduli of carbon and glass tows, respectively. E_{ct} and E_{gt} are obtained from the rule of mixtures based on the moduli of fiber and matrix (Table 1) and fiber/matrix volume fraction. In other words, by applying the rule-of-mixtures twice based on their respective constituents, one can obtain the modulus of hybrid composite. The results demonstrate that there is no synergistic effect of the hybridization on the modulus. Similar findings on the modulus through experimental studies were reported in the literature [22]. Although, it is unnecessary to compare a numerical model with the rule-of-mixtures for the evaluation of longitudinal modulus, the good agreement in the results indicated in Fig. 7 validates the computer program. This program is subsequently used for simulations to predict the tensile strength of unidirectional hybrid composites.

In principle, the carbon tows (strain at failure $\approx 1.1\%$ – obtained from both experiments and simulations on a carbon-tow based composites) cannot elongate as much as the glass tows (strain at failure $\approx 2.0\%$), thus the carbon tows initiate local failure in the hybrid composite. In our proposed tow-based model (a two-phase model) for the Monte-Carlo simulation, the hybrid composite strength can be related to the properties of the carbon and glass tows in the same way that the non-hybrid composite strength can be related to the properties of the fiber and matrix. Therefore, similar to the relationship set up for non-hybrid composites [20], we propose to express the strength of the hybrid composite (S_h) as

$$S_h = S_c\alpha + (\sigma_g)_{\varepsilon@1.1\%}(1-\alpha), \tag{19}$$

where S_c is the carbon/epoxy tow strength; $(\sigma_g)_{\varepsilon@\ 1.1\%}$ is the stress state of glass/epoxy composite at 1.1% of strain (ε), which corresponds to the strain at failure of carbon tow. For small values of the hybrid composition (α), there may not be enough carbon tows to cause failure of the hybrid composite. In such cases, S_h should be governed by the strength of glass/epoxy composite (S_g) and should be approximated by:

$$S_h = S_g(1-\alpha). \tag{20}$$

It should be noted that S_h, S_c and S_g correspond to the same volume fraction of resin. And the minimum hybrid composition (α_{min}) for the validity of Eq. (19), which can be obtained from:

$$\alpha_{min} = \frac{S_g - (\sigma_g)_{\varepsilon@1.1\%}}{S_c + S_g - (\sigma_g)_{\varepsilon@1.1\%}}. \tag{21}$$

By imposing the condition $S_h > S_g$, one can attain the critical hybrid composition (α_{cr}) that must be exceeded in order to gain the hybrid reinforcement:

$$\alpha_{cr} = \frac{S_g - (\sigma_g)_{\varepsilon@1.1\%}}{S_c - (\sigma_g)_{\varepsilon@1.1\%}}. \tag{22}$$

Fig. 8(a) displays the predicted strengths of hybrid composite resulted from Eqs. (19) and (20) as a function of hybrid composition (two segmented solid lines; the epoxy volume fraction was assumed to be 40%). The composite strengths for α equivalent to 0% and 100% match the strengths of GFRP (0.97 GPa) and CFRP (1.52 GPa), respectively. The hybrid composition corresponds to the intersection of these two solid lines is α_{min}. Also shown in Fig. 8(a) are the simulated results (symbols). The graphical displays of the strength variability for these symbols are the outcome from the statistical geometry distribution of tows in the simulation, which will be discussed later. From the results in Fig. 8(a), in general, there is a consistent trend between the analytically predicted and simulated tensile strengths. The results (either from the prediction or the simulation) indicate that the tensile strength of hybrid composites is lower than that of the glass/epoxy composite (non-hybrid) for small values of α (say $\alpha < \alpha_{min}$). In such a hybrid composite, the elongation is controlled by the glass-tow elongation, and all carbon tows break due to the large hybrid composite elongation (Fig. 8(b)). Accordingly, the strength of the hybrid composite is

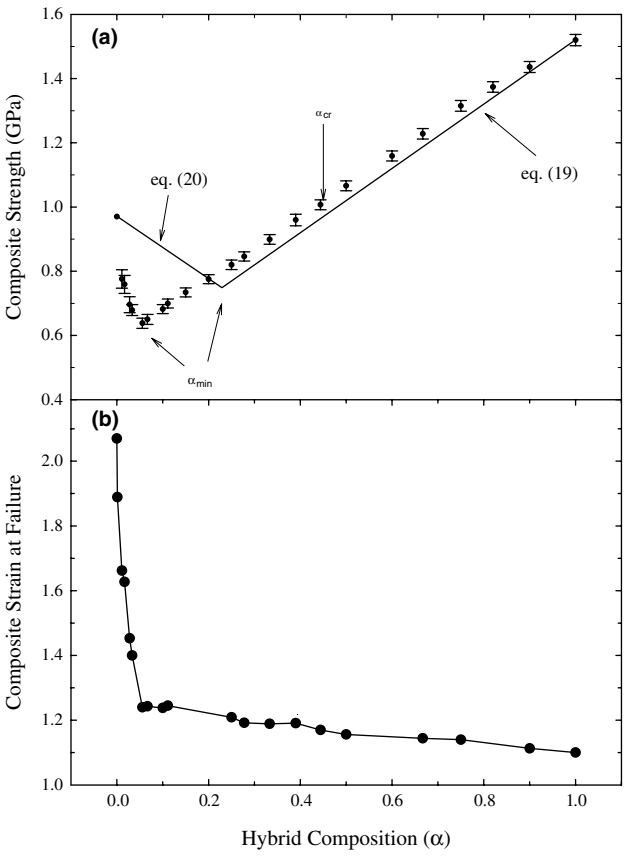

Fig. 8. The predicted strengths of hybrid composite from the analytical model and Eqs. (19) and (20) as a function of hybrid composition (a), the corresponding strain at failure (b). The error bars represent the standard uncertainty from a distribution of results due to the statistical geometry distribution of tows.

actually controlled by the strength of the glass tows. Consequently, as shown in Fig. 8(a), the hybrid composite strength decreases as α increases (because the glass-tow fraction is decreasing). Although the elongation of the hybrid composite is controlled by the elongation of carbon tows when $\alpha_{min} < \alpha < \alpha_{cr}$ (Fig. 8(b)), the tensile strength of the stiffened hybrid composite is still lower than the inherent strength of a non-hybrid glass/epoxy composite. When $\alpha > \alpha_{cr}$, the hybrid composite gains strength over a non-hybrid glass/epoxy composite from having enough carbon-tow reinforcement.

The value of α_{min} from the simulation is a smaller value ($\approx$0.05) than the predicted value ($\approx$0.25) obtained from Eq. (21), and the simulated strength is significantly lower than the predicted strength when $\alpha < 0.25$. This is due to the consideration of stress concentrations in the simulation not accounted for in the prediction. These stress concentrations are induced by the carbon-fiber breakage at relatively low strain. Therefore, the randomly distributed carbon tows in a glass-tow dominated composite act as randomly distributed flaws in the composite. These flaws are the nucleation sites for glass-tow failure at a low level of loading (deformation). Also, it is noticeable that there is reasonably good agreement between the predicted and simulated strengths of the hybrid composite when $\alpha > 0.25$. Consequently, there is virtually no discrepancy between the values of the predicted and simulated α_{cr}. The slight discrepancy between the simulated and the predicted strengths results from the interfacial shear strength between tows and the statistical distribution of tow strength in the simulation.

Recall that the hybrid composite used in this study contains fiber tows randomly placed rather than being packed in a regular pattern as shown in Fig. 2. Therefore, similarly to the statistical strength distribution of the carbon tow, in the simulation the arrangement of carbon and glass tows in the hybrid composite was also set into a random array according to the Monte-Carlo method (a statistical geometry distribution). A typical cross-section of a composite with a random array of tows was shown in Fig. 9. It is found that the coefficient of variation (ratio of the average strength dispersion to the average strength) of twenty random arrangements of tows is less than 1% (Fig. 8(a)). This implies that the strength of a hybrid composite is not sensitive to the random arrangement of tows, and also indicates that tows do not interact strongly (no synergistic effect), so that the strength of a hybrid composite should follow a simple rule-of-mixtures.

In order to make our findings more general, the effect of matrix volume fraction on the hybrid composite strength is also examined using the Monte-Carlo simulation. Fig. 10 displays the variation of tensile strength with matrix volume fraction for the hybrid compositions equal to 0.05 and 0.5. Also shown in the figure as a reference are the simulated tensile strengths for CFRP and

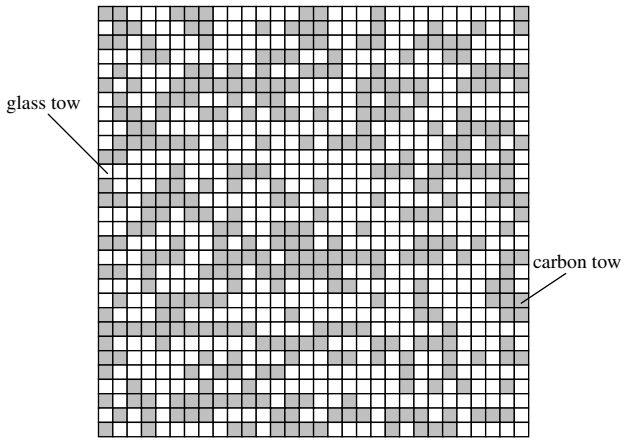

Fig. 9. A typical cross-section of a hybrid composite with random array of carbon and glass tows ($\alpha = 40\%$).

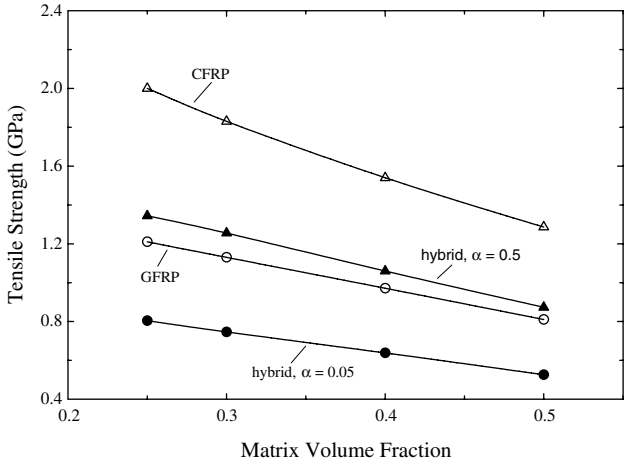

Fig. 10. Simulated tensile strengths as a function of matrix volume fraction for $\alpha = 0$ (GFRP), 0.05, 0.5 and 1 (CFRP).

GFRP composites. One can see from the figure that the composite strength decreases as the matrix volume fraction increases. More importantly, from the parallel trends of the strength (within the uncertainty of simulated results) shown for the non-hybrid composites and the hybrid composites, one can see that the effect of matrix on the composite strength is independent of the hybrid composition. And we can infer that the matrix volume fraction of a hybrid composite does not influence the values of α_{min} and α_{cr} predicted by Eqs. (21) and (22). This further demonstrates that the interactions among tows are simple without any synergistic effect.

4. Conclusions

By mirroring the relationship of fiber/matrix in non-hybrid composites, we have incorporated the rule-

of-mixtures into a tow-based concept to develop an analytical model for predicting the tensile properties (stiffness and strength) of hybrid composites containing different unidirectional fiber tows intimately mixed throughout the composite. A Monte-Carlo method was employed to incorporate a statistical distribution of strength along with a random arrangement of tow geometries to numerically simulate the tensile properties. The tow-based model and simulation treat impregnated tows as minimal microstructures. Also, we have formulated the interfacial shear stress between tows and incorporated it into the simulation. Good agreement between the predictions and simulations on the tensile properties demonstrates the simple interaction among different fiber tows in the hybrid composites – there is no synergistic effect of hybridization on the tensile properties. Consequently, the tensile properties of hybrid composites are well predicted using the rule-of-mixtures. Thus, once constituent properties and volume fractions of tows are determined, the tensile properties of composites with any hybrid content can be calculated.

Notably, that the addition of small amounts of carbon does make the material stiffer, but dramatically reduces the strength of hybrid composites. Also, our study indicates that intraply hybrid has a slightly lower strength than the equivalent random hybrid, as the failures would propagate more rapidly into the adjacent carbon layers causing overall failure at lower strains. Therefore, the random hybrid is in some sense a better choice. Finally, although the study deals solely with glass/carbon hybrid composites, the proposed analytical model for predicting the tensile properties and general observations in the study should be valid for any type of hybrid construction.

References

[1] Oh KP. A Monte-carlo study of the strength of unidirectional fiber-reinforced composite. J Compos Mater 1979;13:311–28.

[2] Goda K, Phoenix SL. Reliability approach to the tensile strength of unidirectional CFRP composites by Monte-Carlo simulation in a shear-lag model. Comp Sci Technol 1994;50:457–68.

[3] Landis CM, Beyerlein IJ, McMeeking RM. Micromechanical simulation of the failure of fiber reinforced composites. J Mech Phys Solid 2000;48:621–48.

[4] Kim JK, Kim CS, Song DY. Strength evaluation and failure analysis of unidirectional composites using Monte-Carlo simulation. Mater Sci Eng A 2003;340:33–40.

[5] Fariborz SJ, Tang CL, Harlow DG. The tensile behavior of intraply hybrid composites I: model and simulation. J Comp Mater 1985;19:334–54.

[6] Fariborz SJ, Harlow DG. The tensile behavior of intraply hybrid composites II: micromechanical model. J Comp Mater 1987;21:856–75.

[7] Okabe T, Takeda N, Kamoshida Y, Shimizu M, Curtin WA. A 3D shear-lag model considering micro-damage and statistical strength prediction of unidirectional fiber-reinforced composites. Comp Sci Technol 2001;61:1773–87.

[8] Curtin WA. Theory of mechanical-properties of ceramic–matrix composites. J Am Ceram Soc 1991;11:2837–45.

[9] Yuan JM, Xia YM, Yang BC. A note on the monte-carlo simulation of the tensile deformation and failure process of unidirectional composites. Comp Sci Technol 1994;52:197–204.

[10] Wang XF, Zhao JH. Monte-Carlo simulation to the tensile mechanical behavior of unidirectional composites at low temperature. Cryogenics 2001;41:683–91.

[11] Ochiai S, Hoj M, Schulte K, Fielder B. A shear-lag approach to the early stage of interfacial failure in the fiber direction in notched two dimensional unidirectional composites. Comp Sci Technol 1997;57:775–85.

[12] Ferziger JH. Numerical methods for engineering application. New York: Wiley; 1981.

[13] Bennett JA, Young RJ. The effect of fiber–matrix adhesion upon crack bridging in fiber reinforced composites. Compos Part A – Appl Sci 1998;29:1071–81.

[14] Chiang MYM, He JM. An analytical assessment of using the losipescu shear test for hybrid composites. Compos Part B – Eng 2002;33:461–70.

[15] Tsai SW. Introduction of composite materials. Micromechanics. West Port, CT: Technomic Publishing Co., Inc.; 1980. p. 388–401 [chapter 9].

[16] He JM, Chiang MYM, Hunston DL, Han CC. Application of the V-notch shear test for unidirectional hybrid composites. J Compos Mater 2002;6:2653–66.

[17] Marston C, Gabbitas B, Adams J. The effect of fibre sizing on fibres and bundle strength in hybrid glass carbon fibre composites. J Mater Sci 1997;32:1415–23.

[18] Zhao FM, Takeda N. Effect of interfacial adhesion and statistical fiber strength on tensile strength of unidirectional glass fiber epoxy composites: Part I. Experiment results and Part II. Comparison with prediction. Composites Part A 2000;31:1215–24.

[19] Kelly A, Davies GJ. The principles of the fibre reinforcement of metals. Metall Rev 1965;10:1–77.

[20] Bader MG, Priest AM. Statistical aspects of the fiber and bundle strength in hybrid composites. In: Hayashi T, Kawata K, Umekawa S, editors. Progress in Science and Engineering Composites ICCM-IV; 1982. p. 1129–1136.

[21] Isida M. On the determination of stress intensity factors for some common structural problems. Eng Fract Mech 1970;2:61.

[22] Marom G, Fischer S. Hybrid effects in composites: conditions for positive or negative effects versus rule-of-mixtures behavior. J Mater Sci 1978;13:1419–26.